Signalling probes appended with two rhodamine derivatives: Inter-component preferences, Fe(III)-ion selective fluorescence responses and bio-imaging in plant species

Debajani Mallick[a,b], Biswonath Biswal[a], M. Thirunavoukkarasu[c], Roshnara Mohanty[c], Bamaprasad Bag[a,b,*]

[a]Colloids and Materials Chemistry Department, [b]Academy of Scientific and Innovative Research, [c]Environment and Sustainability Department, CSIR-Institute of Minerals and Materials Technology, P.O.: R.R.L., Bhubaneswar-751 013, Odisha, India. Email: bpbag@immt.res.in

Supplementary Information

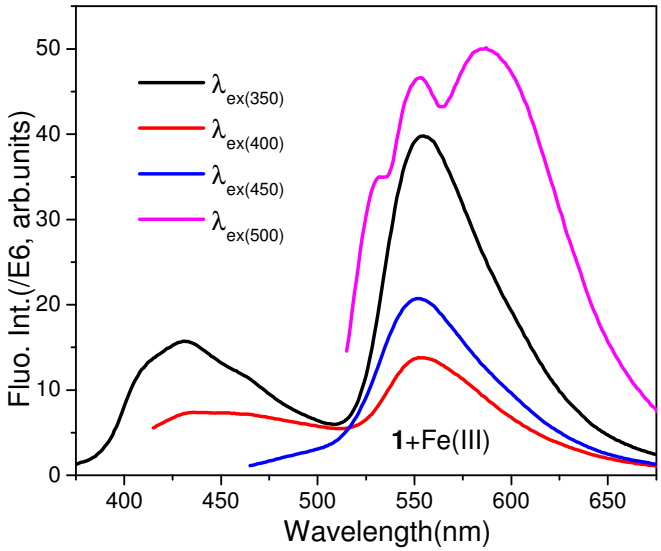

Fig. S1: Fluorescence spectral pattern of **1** in presence of Fe(III) ion in EtOH–H_2O (1:1 v/v, 0.1M PBS) medium on excitation at various wavelength. [**1**] = 1μM, [Fe(III)] = 5 μM, em. and ex. b.p. = 5 nm, RT.

Fig. S2: Photograph of change in colour of the solution of **1** in EtOH–H_2O (1:1 v/v, 0.1M PBS) medium on addition of various metal ions; added metal ions (from left to right: blank, Na(I), K(I), Ca(II), Mn(II), Fe(II), Fe(III), Co(II), Ni(II), Cu(II), Zn(II), Ag(I), Cd(II), Hg(II) and Pb(II).

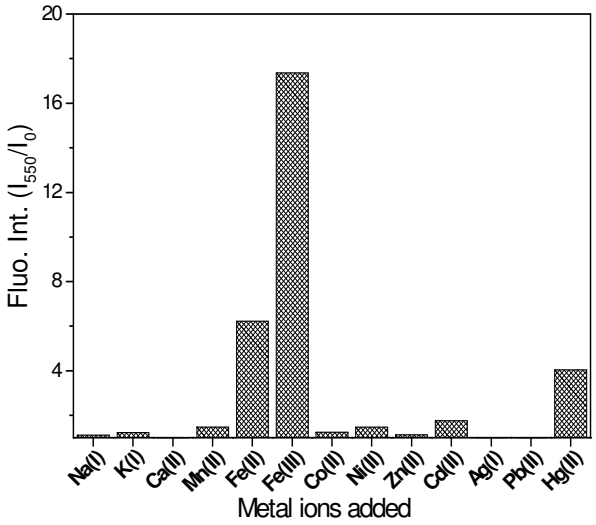

Fig. S3: Fluorescence enhancement factor (I_{550}/I_0) of **1** in presence of various metal ions. [**1**] = 1μM, [M(I/II/III)] = 10 μM, λ_{ex} = 500 nm, em. and ex. b. p. = 5 nm, RT, EtOH.

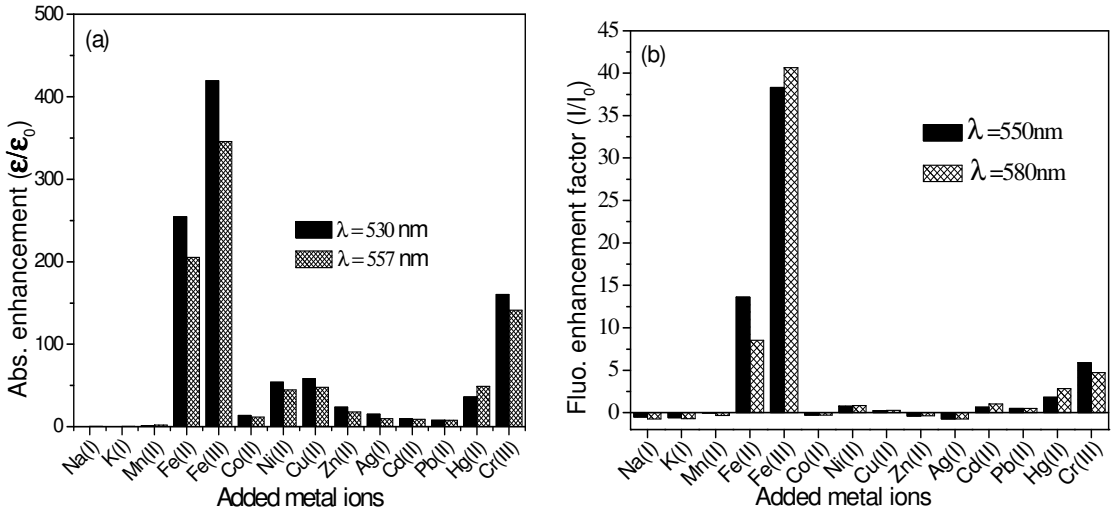

Fig. S4: (a) Absorption enhancement factor ($\varepsilon/\varepsilon_0$) and (b) Fluorescence enhancement factor (I_{550}/I_0) of **2** in presence of various metal ions in EtOH-H_2O(1:1 v/v, 0.1M PBS) medium. Abs: [**2**] = 10μM, [M(I/II/III)] = 25 μM; Fluorescence: [**2**] = 1μM, [M(I/II/III)] = 5 μM; λ_{ex} = 500 nm, em. and ex. b. p. = 5 nm, RT.

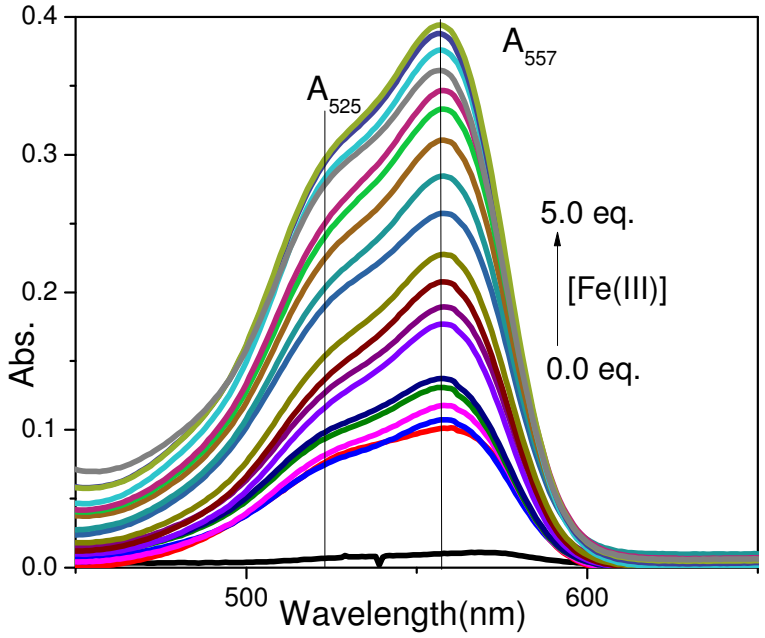

Fig. S5: Absorption titration spectra of **1** as a function of added Fe(III) ion. The spectra were recorded 3h after addition of solutions of metal ions to that of probes. [**1**] = 6.6 μM. The increase in A_{557} peak in comparison to A_{525} peak in the spectra shows coordination pattern of Rho-B component becomes predominant over Rho-6G component over time.

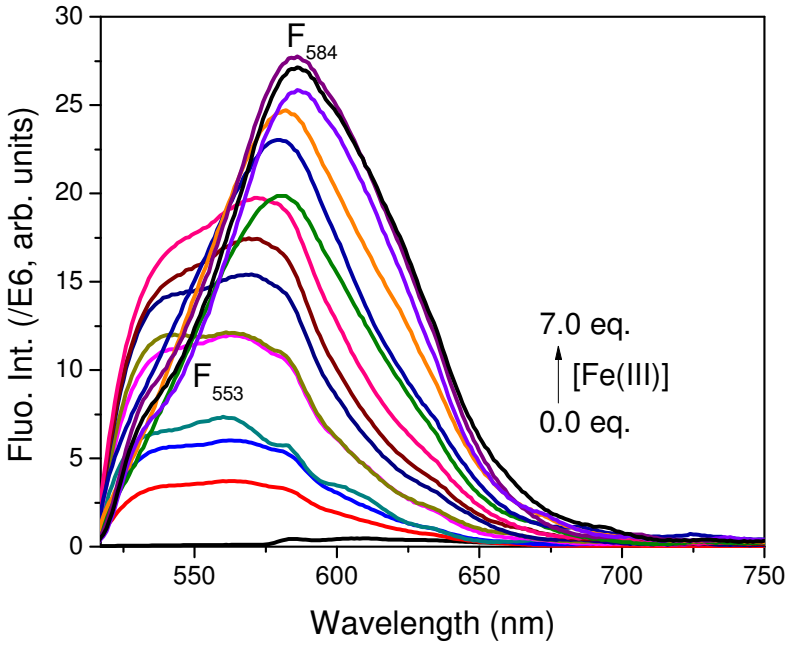

Fig. S6: Fluorescence titration spectra of **1** as a function of added Fe(III) ion. The spectra were recorded 3h after addition of solutions of metal ions to that of probes. The increase in F_{580} peak in comparison to F_{550} peak in the spectra shows coordination pattern of the probe's Rho-B component becomes predominant over Rho-6G component over time. [**1**] = 1μM, λ_{ex} = 500 nm, em. and ex. b.p. = 5 nm, RT.

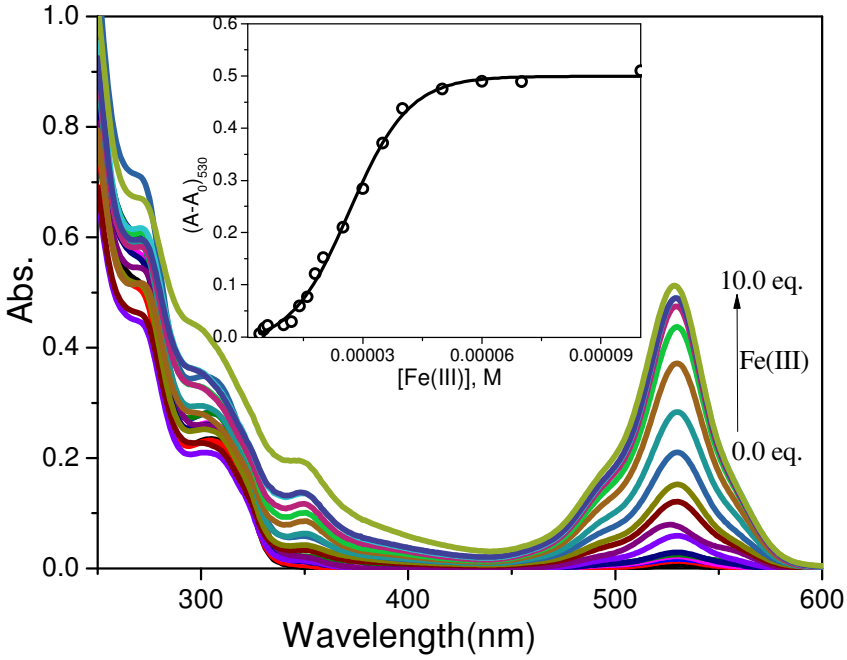

Fig. S7: Absorption titration spectra of **2**(10μM) as a function of added Fe(III) ion in EtOH-H_2O(1:1v/v, 0.1M PBS) medium. Inset: Absorption intensity change ($A-A_0$) at 530 nm versus added concentration of Fe(III) ion.

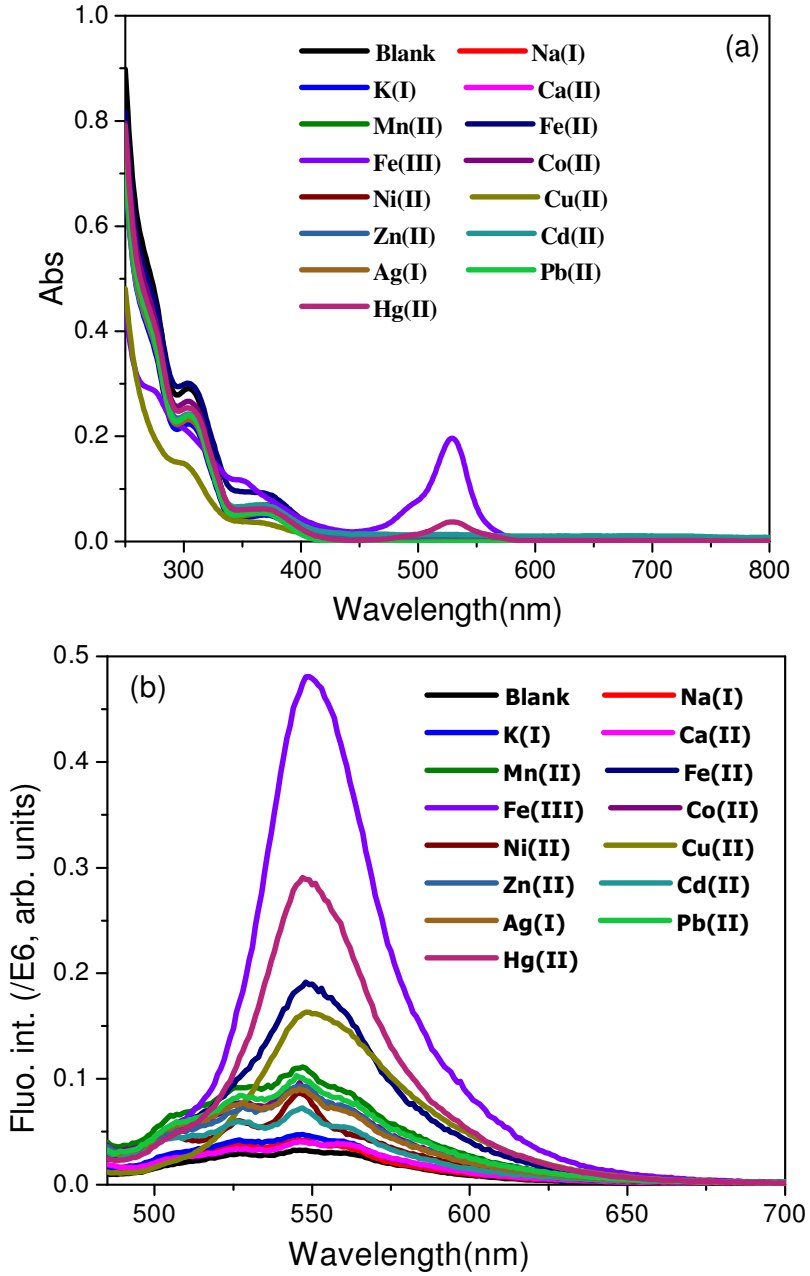

Fig S8: (a): Absorption and (b) fluorescence spectra of **1** in presence of metal ions in **MeCN–H_2O** (9:1 v/v, PBS, 0.1M) medium. λ_{ex} = 470 nm, em. and ex b. p. = 5 nm, RT. The spectral pattern in different solvent/binary mixture medium shows that Fe(III) ion exhibited optimal absorption and fluorescence spectral responses in **1** among various metal ions due to higher probe-metal interaction irrespective of solvent condition (those investigated here).

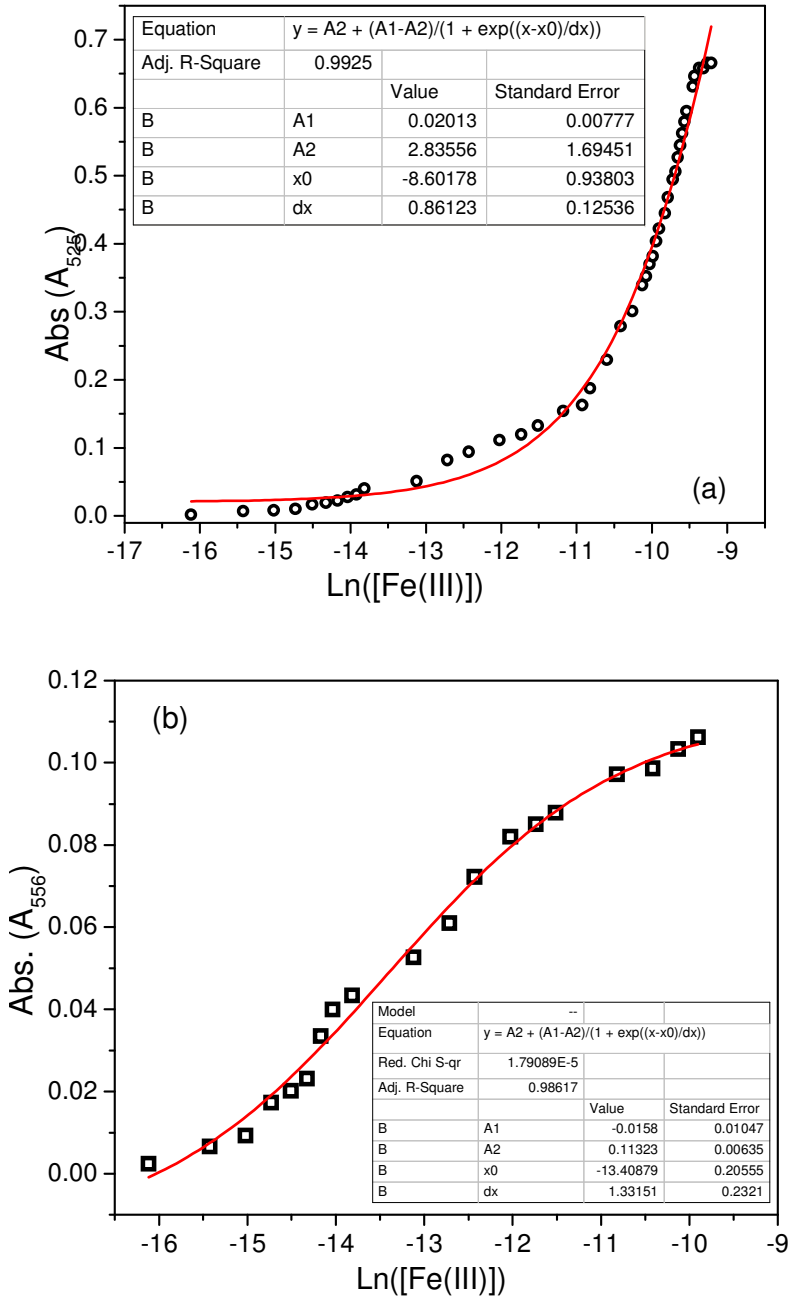

Fig. S9: Non-linear regression plot of complex **1**-Fe(III) for determination of association constant (Ka). The absorption data taken at (a) 525nm and (b) 556 nm from the titration of **1** as a function of added Fe(III) ion.

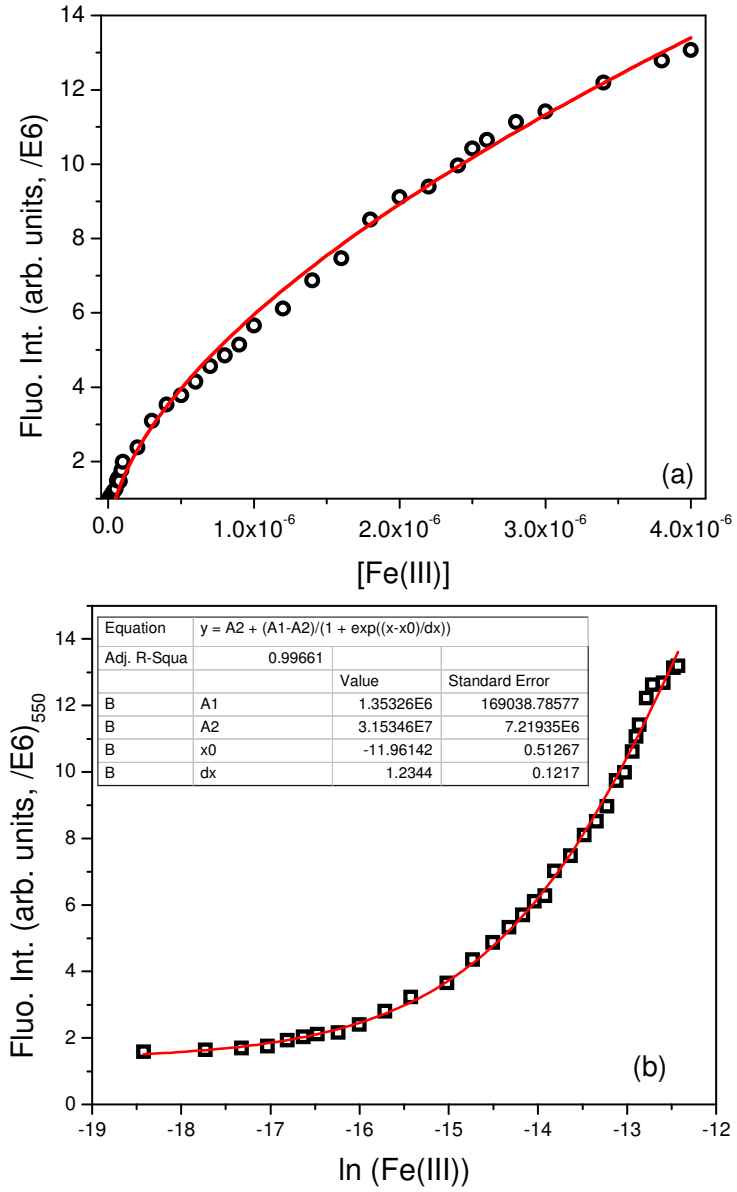

Fig. S10: Non-linear regression plot of complex **1**-Fe(III) for determination of association constant (Ka) through fluorescence titration. (a) The fluorescence intensity data taken at 550 nm (a) as a function of added Fe(III) ion or (b) ln(Fe(III)). [**1**] = 1μM, λ_{ex} = 500 nm, em. and ex. b. p. = 5 nm, RT.

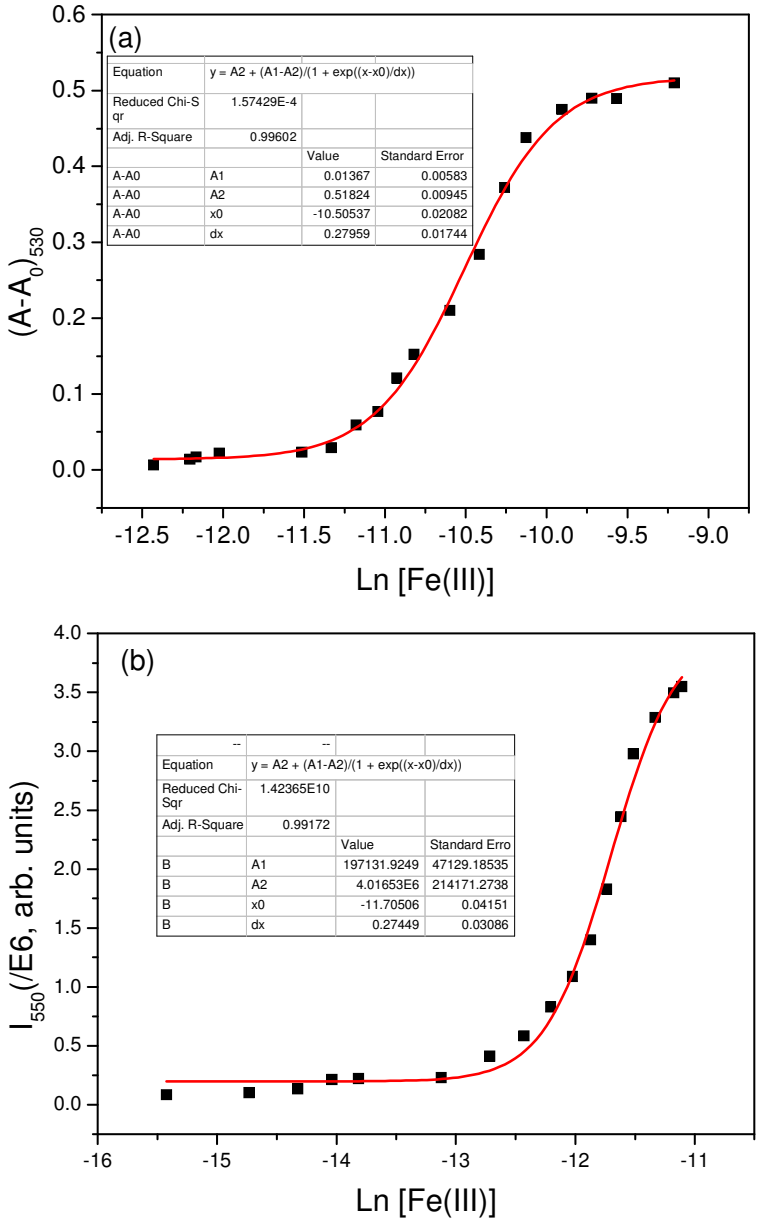

Fig. S11: Non-linear regression plot of change in (a) absorption at 530nm and (b) fluorescence at 550nm of **2** on addition of Fe(III) determination of association constant (Ka). Abs: [**2**] = 10μM, Fluorescence: [**2**] = 1μM, λ_{ex} = 500 nm, em. and ex. b. p. = 5 nm, RT.

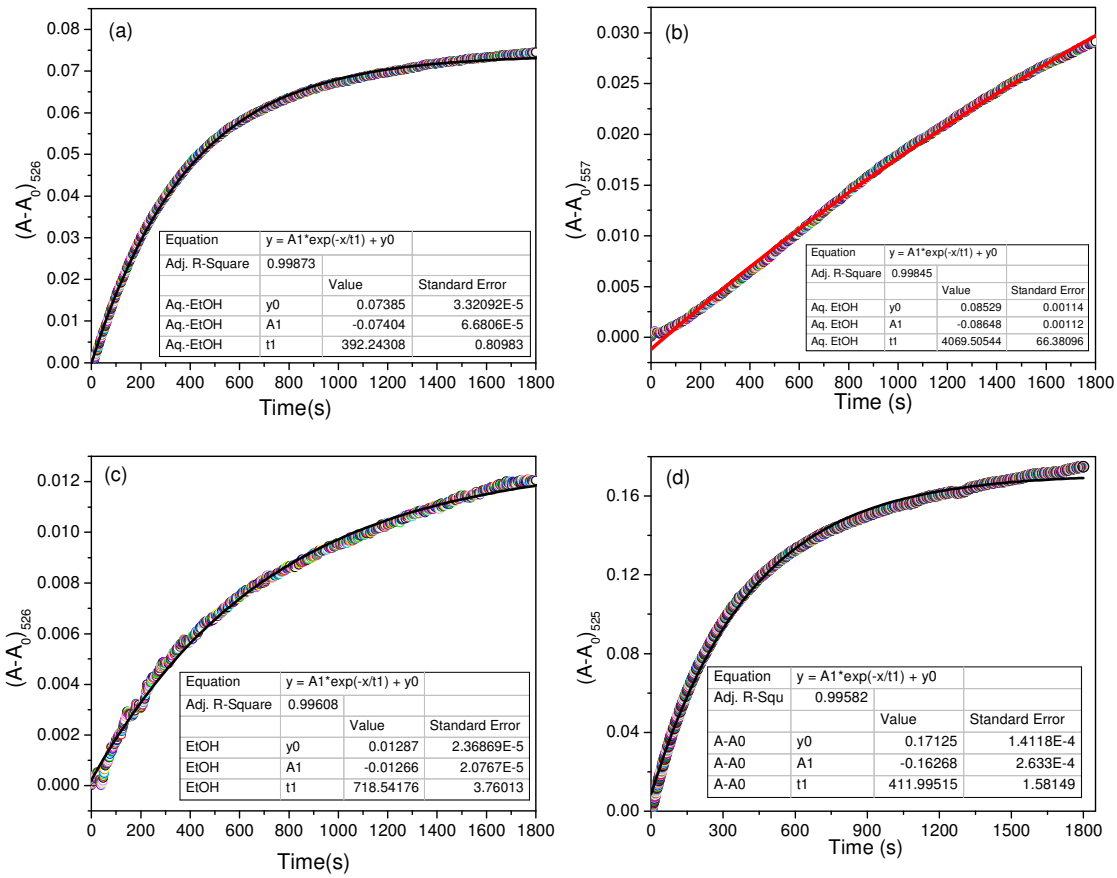

Fig S12: Change in absorption at (a) 525nm(A_{525}), (b) 557nm(A_{557}) in **1**(5μM) on equimolar Fe(III) ion addition as a function of time(s) in EtOH–H_2O (1:1 v/v, PBS, 0.1M) medium. (c) The same(A_{525}) when carried out in EtOH medium. [**1**] = [Fe(III)] = 5 μM. (d) Change in absorption(A_{525}) in **1**(10μM) on addition of Fe(III) as a function of time(s) in EtOH–H_2O (1:1v/v, PBS, 0.1M) medium, [**1**] = [Fe(III)] = 10 μM. The non-linear regression fit ($A = A_0 e^{-kt}$) of first-order kinetics at desired time interval determines of rate constant (k).

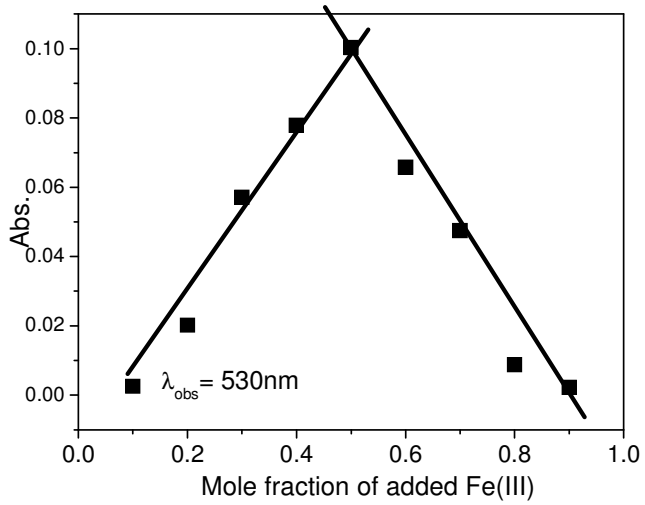

Fig S13: Absorbance of **2** as a function of mole fraction of added Fe(III) ion for determination of complexation stoichiometry.

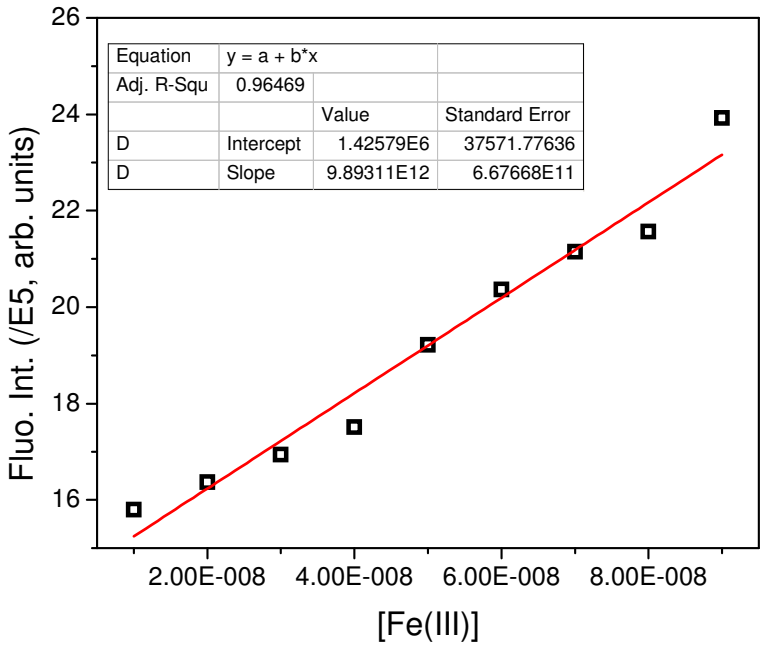

Fig. S14: Linear regression to the plot of fluorescence intensity (I_F/I_0) of **1** (1μM) as a function of concentration of Fe(III) added. (S/N = 5), [**1**] = 1μM, λ_{ex} = 500 nm, em. and ex. b. p. = 5 nm, RT.

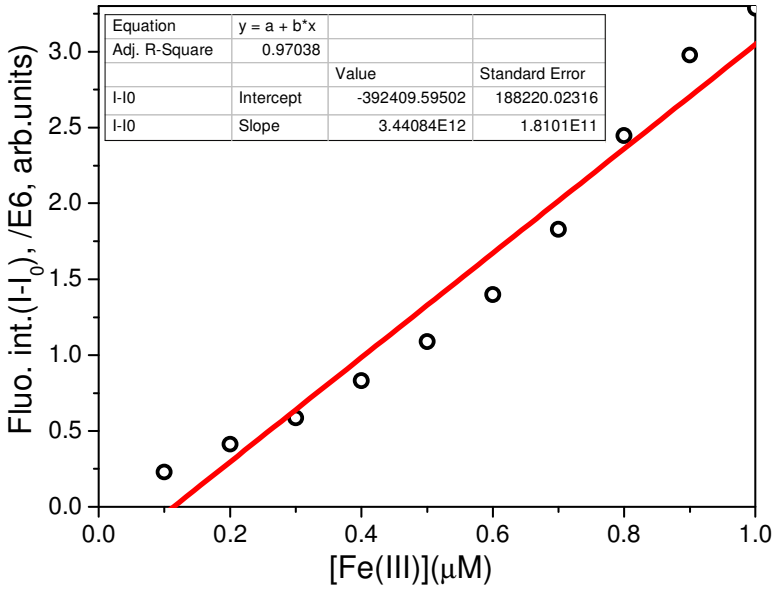

Fig. S15: Linear regression to the plot of fluorescence intensity $(I_F\text{-}I_0)_{550}$ of **2**(1μM) as a function of concentration of Fe(III) added. (S/N = 5), [**2**] = 1μM, λ_{ex} = 500 nm, em. and ex. b. p. = 5 nm, RT.

Table ST1: Comparison in sensitivity among few rhodamine based probes towards detection of Fe(III) ion.

No.	Probe	Sensitivity, LOD	References
1	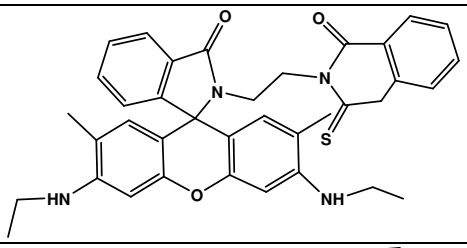	4.11 μM	Y. Wang, H. Chang, W. Wu, X. Zhaoa, Y. Yang, Z. Xu, Z. H. Xu and L. Jia. *Sens. Actuat. B*, 2017,**239**, 60.
2	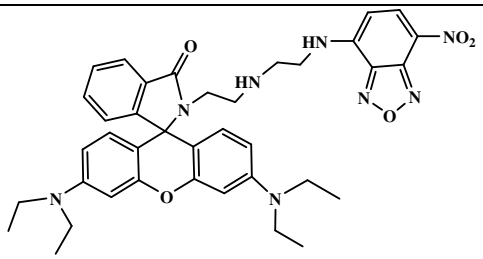	0.1μM	X. Li, Y. Yin, J. Deng, H. Zhong, J. Tang, Z. Chen, L.Yang and L. -J. Ma. *Talanta*, 2016, **154**, 329.
3	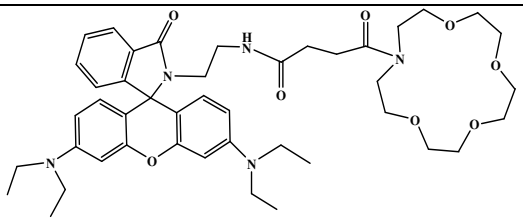	0.396μM	X. Bao, X. Cao, X. Nie, Y. Xu, W. Guo, B. Zhou, L. Zhang, H. Liao and T. Pang, *Sens. Actuat. B*, 2015, **208**, 54.
4	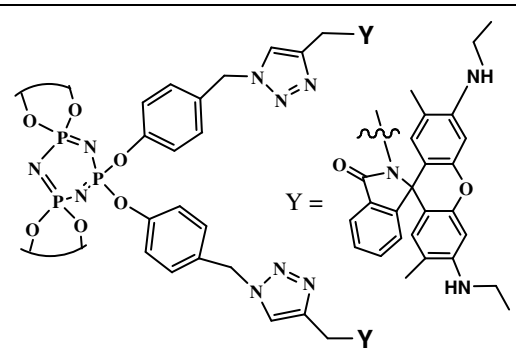	4.8 μM	R. Kagit, M. Yildirim, O. Ozay, S. Yesilot and H. Oza. *Inorg. Chem.*, 2014, **53**, 2144.
5	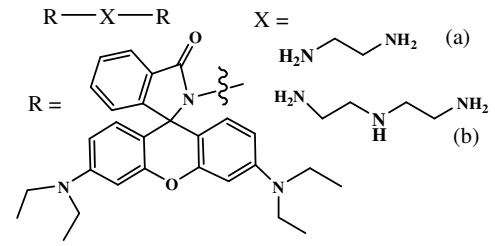	(a) 0.3 μM (b) 1.2 μM	(a) Y. Du, M. Chen, Y. Zhang, F. Luo, C. He, M. Li and X. Chen, *Talanta*, 2013, **106**, 261. (b) Y. Ding, H. Zhu, X. Zhang, J.-J. Zhu and C. Burda, *Chem. Commun.*, 2013, **49**, 7797.
6	Probe **1**	**11nM**	**Work in this manuscript**
7	Probe **2**	**0.16μM**	**Work in this manuscript**

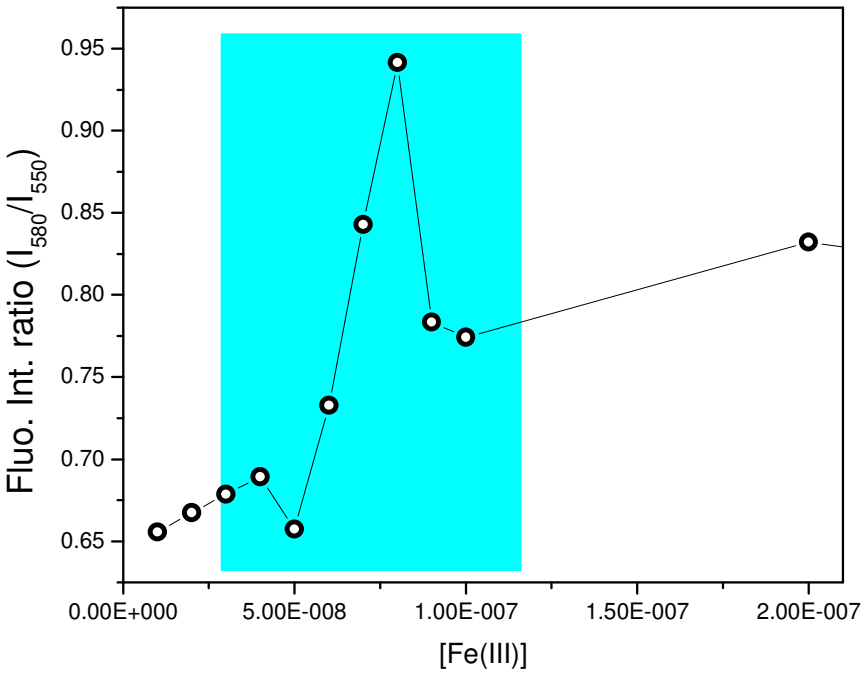

Fig. S16: the plot of fluorescence intensity ratio $[(I_F/I_0)_{580}/(I_F/I_0)_{550}]$ of **1** (1μM) as a function of concentration of Fe(III) added. (S/N = 5), [**1**] = 1μM, λ_{ex} = 500 nm, em. and ex. b. p. = 5 nm, RT.

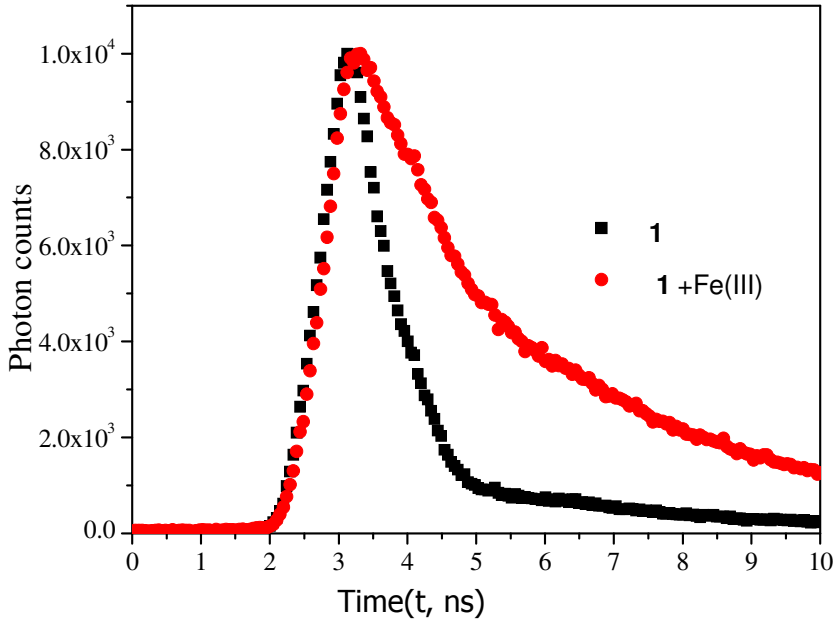

Fig S17: Time-resolved fluorescence exponentially fitted decay profile of **1** alone and in presence of Fe(III) ion in EtOH-H_2O (1:1 v/v, 0.1M PBS) medium.

Table ST 2: Data of the fitted decay profile of **1** and [**1**+Fe(III)]

Fit Results

Fit : $A+B1\exp(-t/\tau_1)+B2\exp(-t/\tau_2)+B3\exp(-t/\tau_3)$

Parameter	Value	Std. Dev.	Rel %
τ_1	1.014E-010 s	8.7554E-012 s	
τ_2	2.648E-009 s	7.2340E-011 s	
τ_3	5.659E-009 s	1.6625E-010 s	
Shift	7.283E-011 s	6.572E-012 s	
B1	0.331	0.0279	26.88
B2	0.019	0.0006	40.92
B3	0.007	0.0007	32.20
A	61.551		
χ^2	1.195		

1

Parameter	Value	Std. Dev.	Rel %
τ_1	6.643E-011 s	1.4727E-011 s	
τ_2	3.184E-009 s	8.5530E-011 s	
τ_3	5.619E-009 s	4.3265E-010 s	
Shift	-1.069E-011 s	1.281E-011 s	
B1	0.451	0.0957	20.91
B2	0.028	0.0016	61.09
B3	0.005	0.0017	18.00
A	54.589		
χ^2	1.107		

1 + Fe(III)

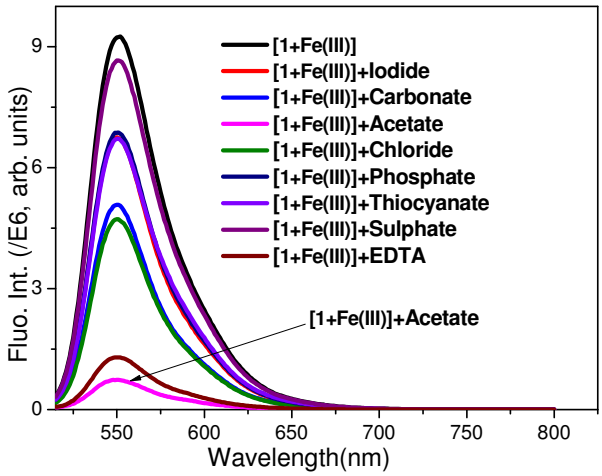

Fig. S18: Fluorescence spectra of [**1**-Fe(III)] *in-situ* complex in presence of various anions and counter reagents. : [**1**] = 1μM, [Fe(III)] = 5μM, [anion] = 10 μM, λ_{ex} = 500 nm, em. and ex. b. p. = 5 nm, RT.

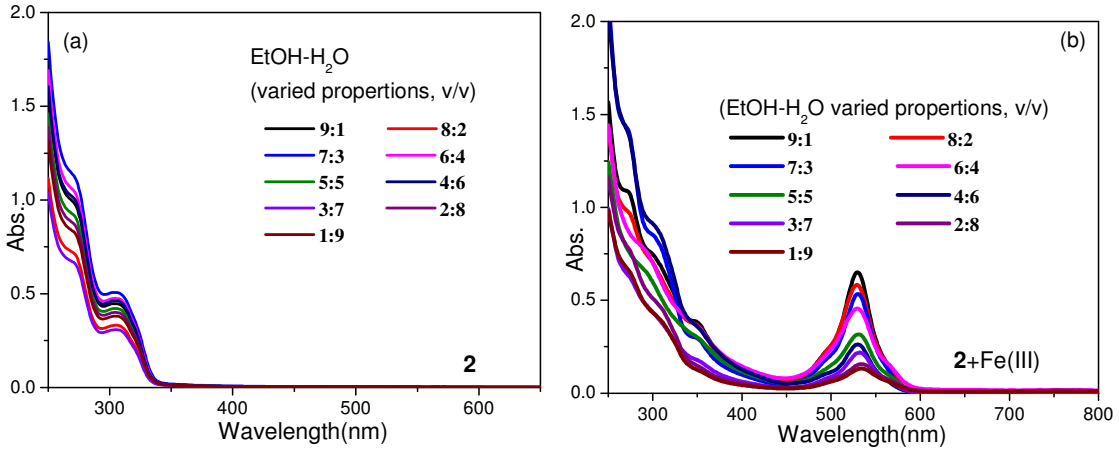

Fig. S19: Absorption spectra of **2** (a) alone and (b) in presence of Fe(III) in varied proportion of a EtOH-H_2O binary mixture (v/v) as solvent medium. [**2**] = 1×10^{-5}M, [Fe(III)] = 5×10^{-5}M.

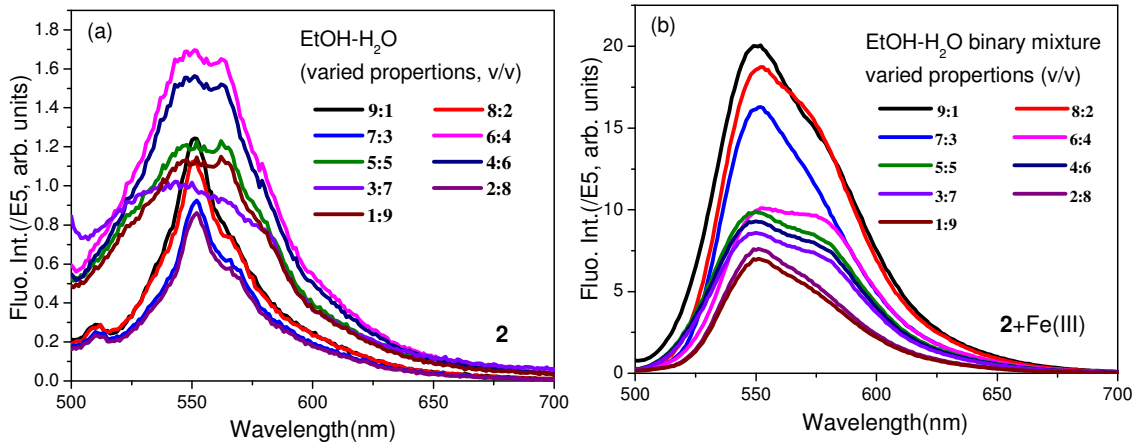

Fig. S20: Fluorescence spectra of **2** alone (a) and (b) in presence of Fe(III) in varied proportion of a EtOH-H_2O binary mixture (v/v) as solvent medium. [**2**] = 1×10^{-6}M, [Fe(III)] = 5×10^{-6}M, λ_{ex} = 480 nm, emission and excitation band pass = 5nm, RT. The error in fluorescence output (for 3 measurements) is < 10 % for ligand and < 5% for the complex.

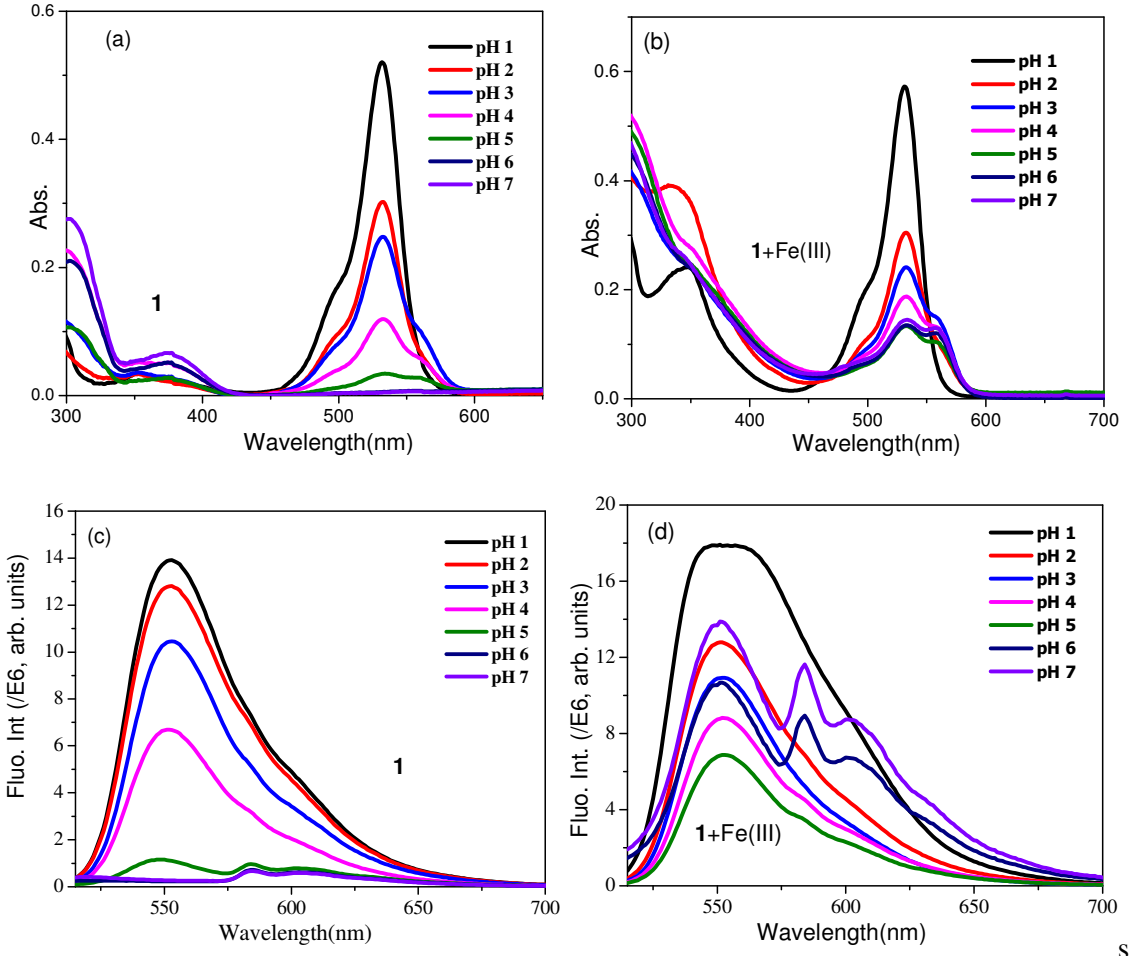

s

Fig. S21: Absorption (a and b) and fluorescence(c and d) spectra of **1**(a and c) and **1**+Fe(III) (b and d) respectively as a function of varying pH in the acidic region. *Conditions*: EtOH–H_2O (1:1 v/v), Abs: [**1**] = 10μM, [Fe(III)] = 20μM, Fluorescence: [**1**] = 1μM, [Fe(III)] = 5μM, λ_{ex} = 500 nm, em. and ex. b. p. = 5 nm, RT.

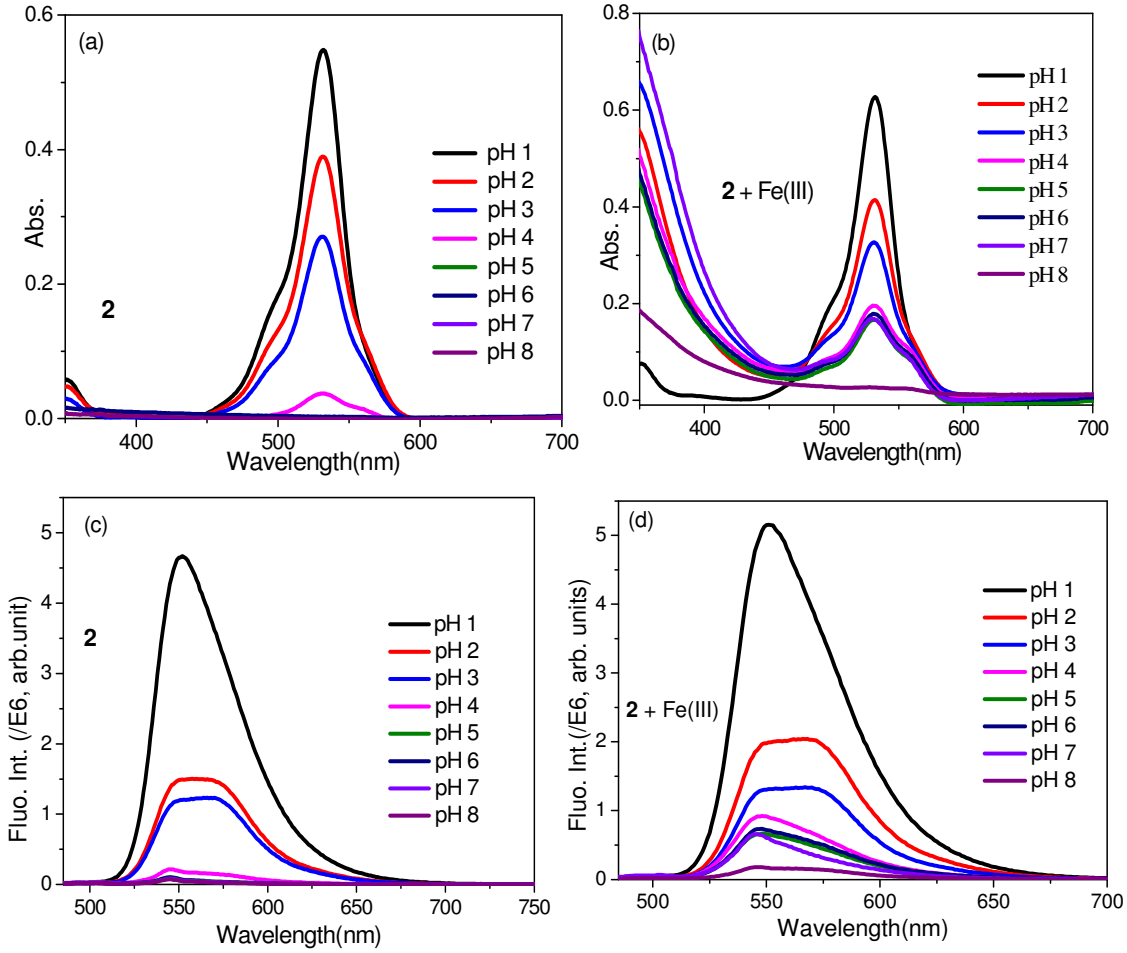

Fig. S22: Absorption (a and b) and fluorescence(c and d) spectra of **2**(a and c) and **2**+Fe(III) (b and d) respectively as a function of varying pH in the acidic region. *Conditions*: EtOH–H_2O (1:1 v/v), Abs: [**2**] = 10μM, [Fe(III)] = 25μM, Fluorescence: [**1**] = 1μM, [Fe(III)] = 5μM, λ_{ex} = 500 nm, em. and ex. b. p. = 5 nm, RT.

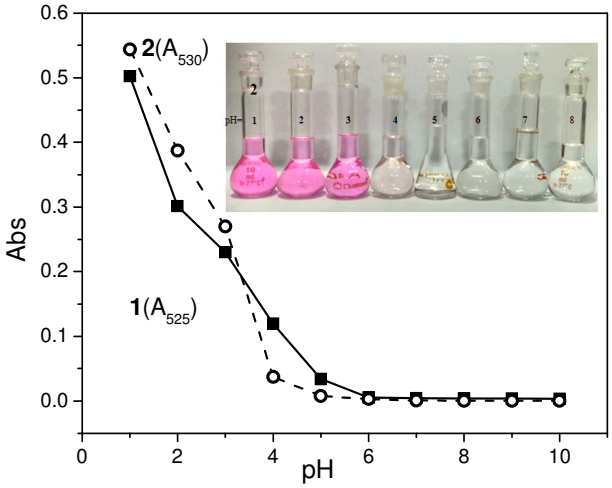

Fig. S23: Comparison of absorption intensities of **1** and **2** as a function of varying pH in the acidic region. Inset: photograph of 2 in EtOH–H_2O (1:1 v/v) at different pH.

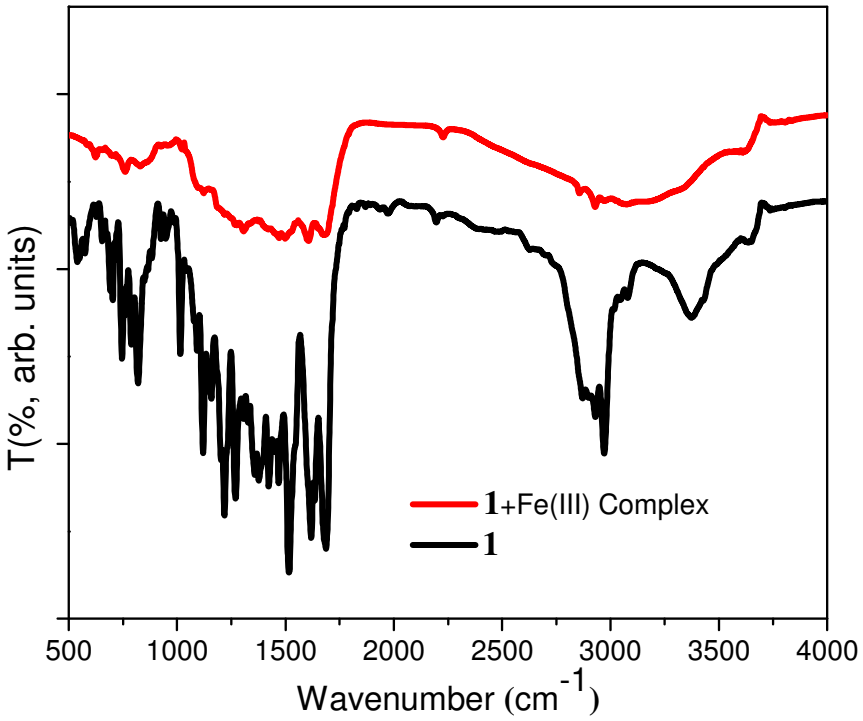

Fig S24: FTIR spectrum of **1** and [**1**+Fe(III)] complex.

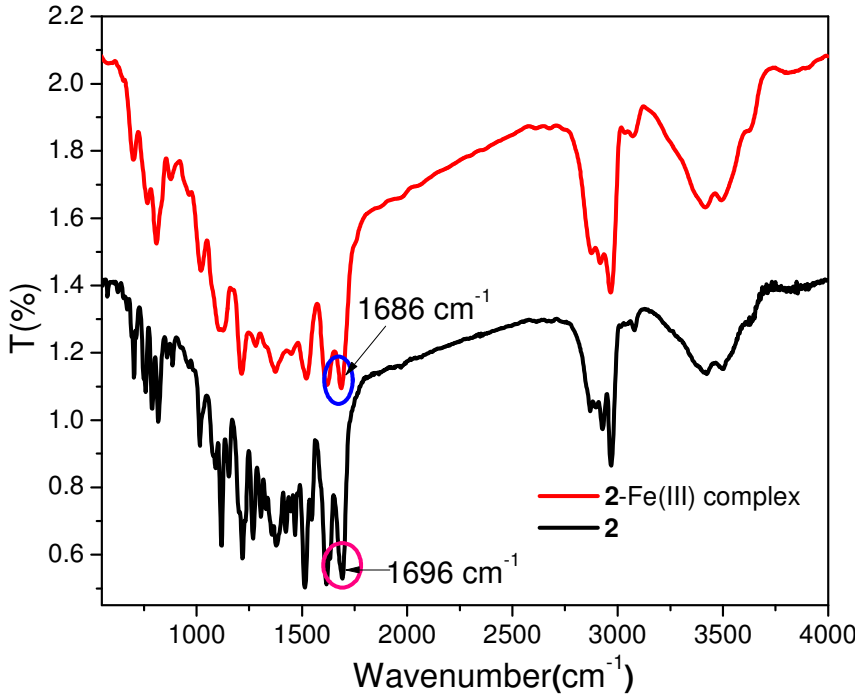

Fig S25: FTIR spectrum of **2** and [**2**+Fe(III)] complex

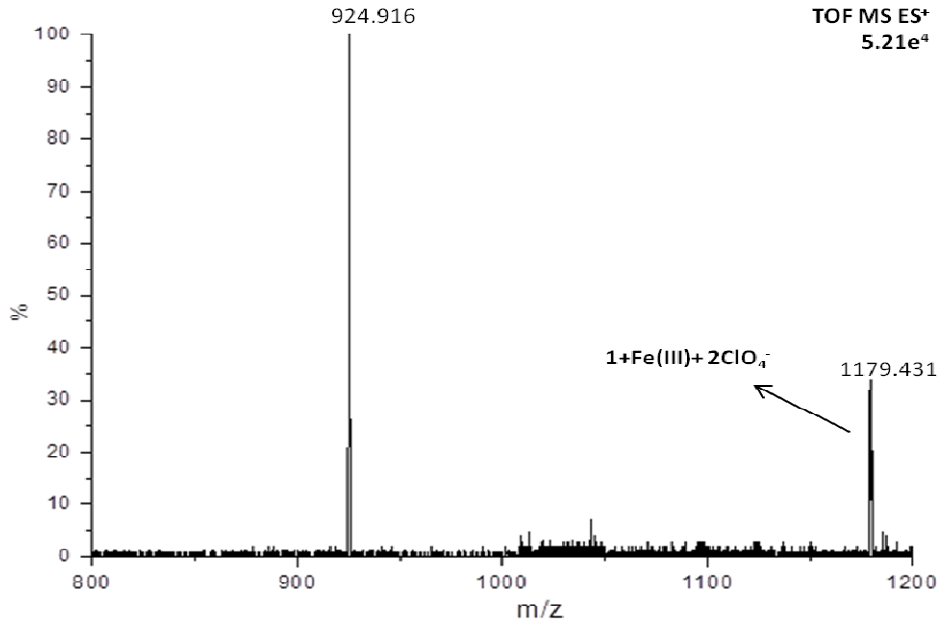

Fig S26: ESI-MS spectrum of complex (**1**+Fe(III)).

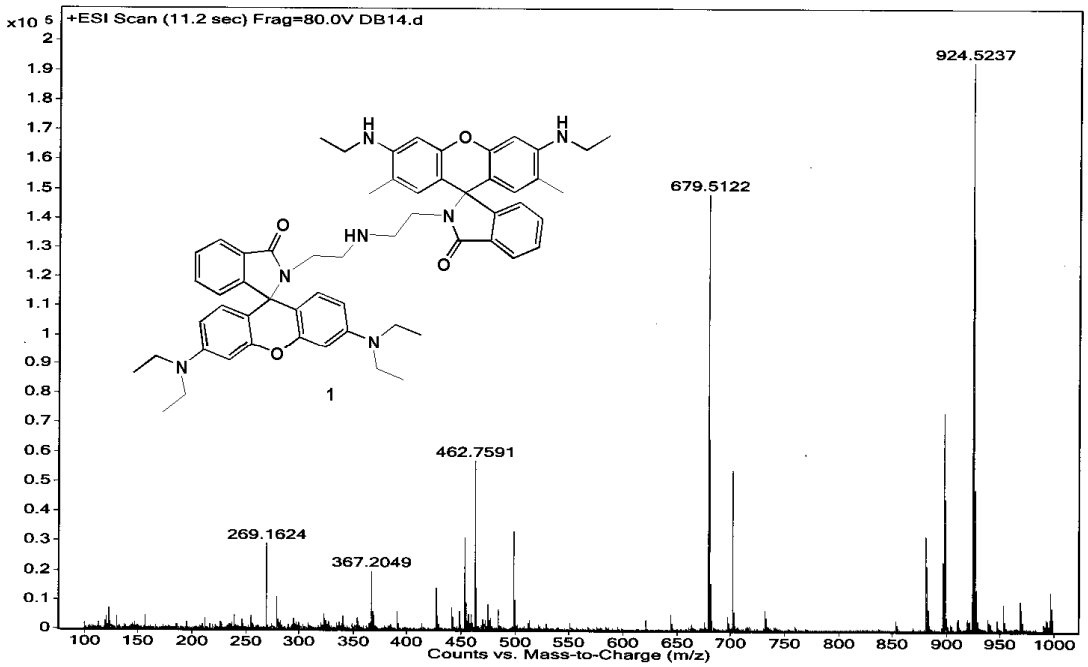

Fig S27: ESI-MS spectrum of **1** (M_w: 923.51).

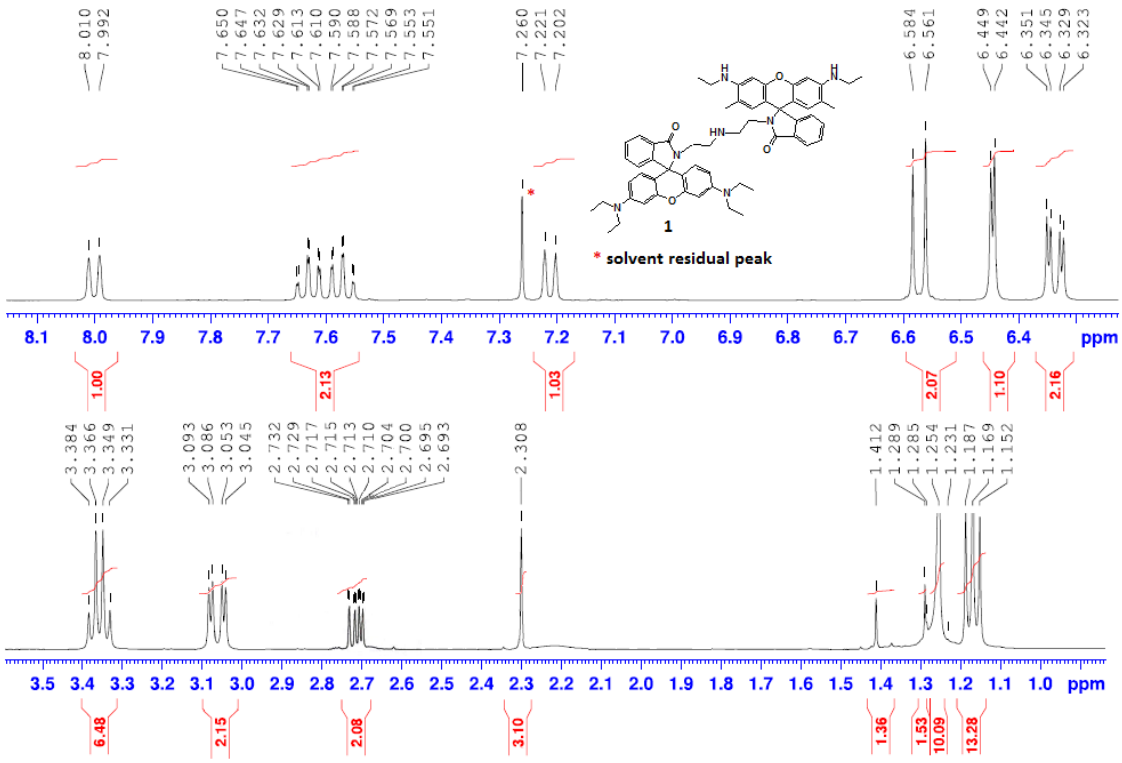

Fig S28: ^{1}HNMR spectrum of **1**($CDCl_3$).

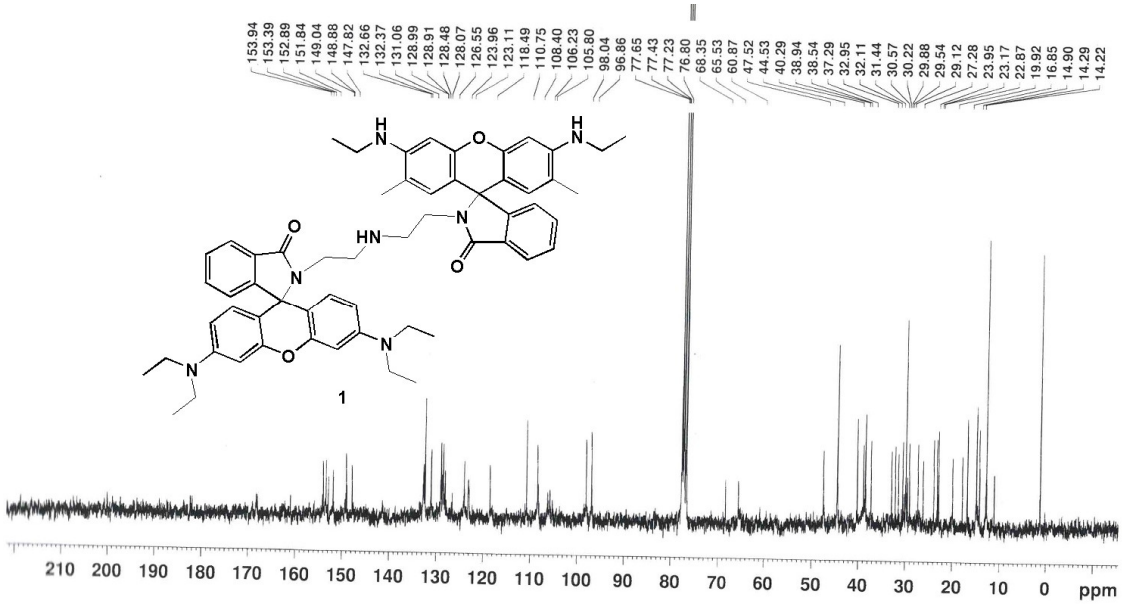

Fig S29: ^{13}C-NMR spectrum of **1**($CDCl_3$).

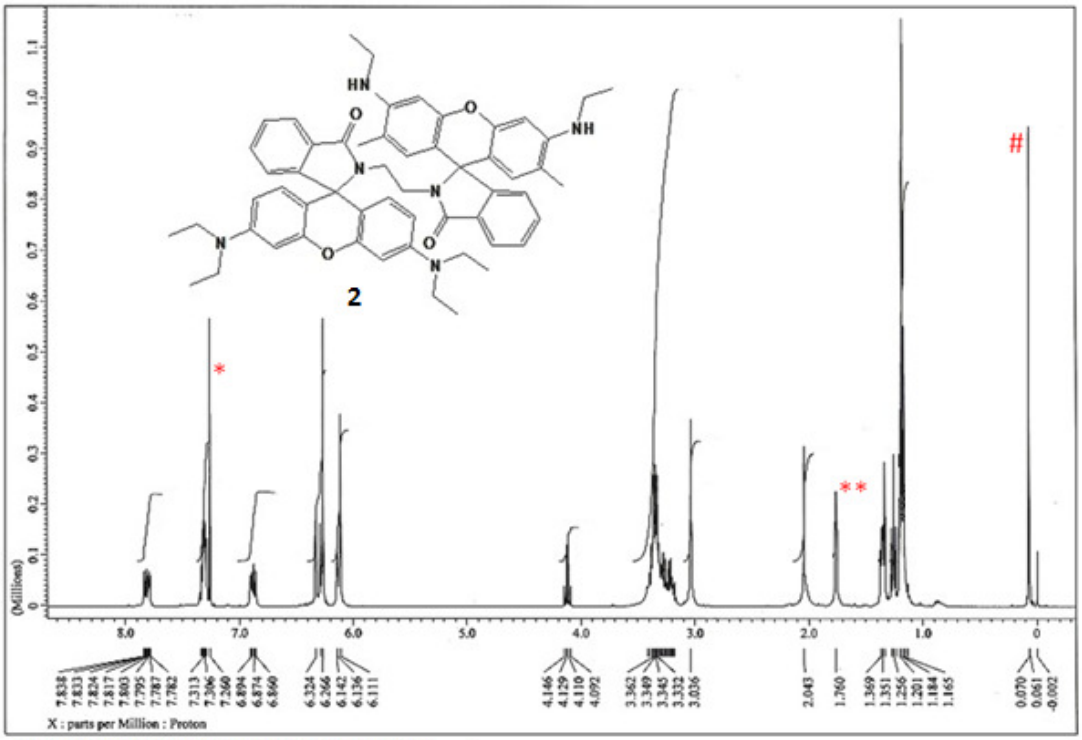

* Solvent residual peak; ** H_2O in $CDCl_3$; # TMS

Fig S30: ^{1}HNMR spectrum of **2**($CDCl_3$).

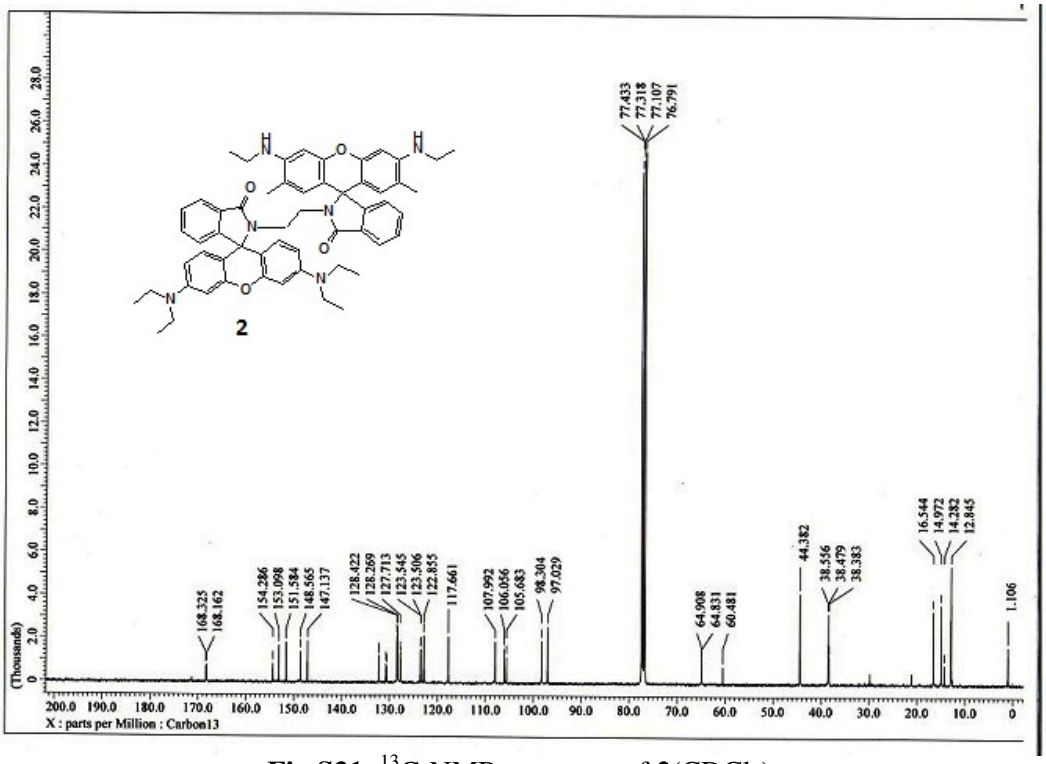

Fig S31: ^{13}C-NMR spectrum of **2**($CDCl_3$).

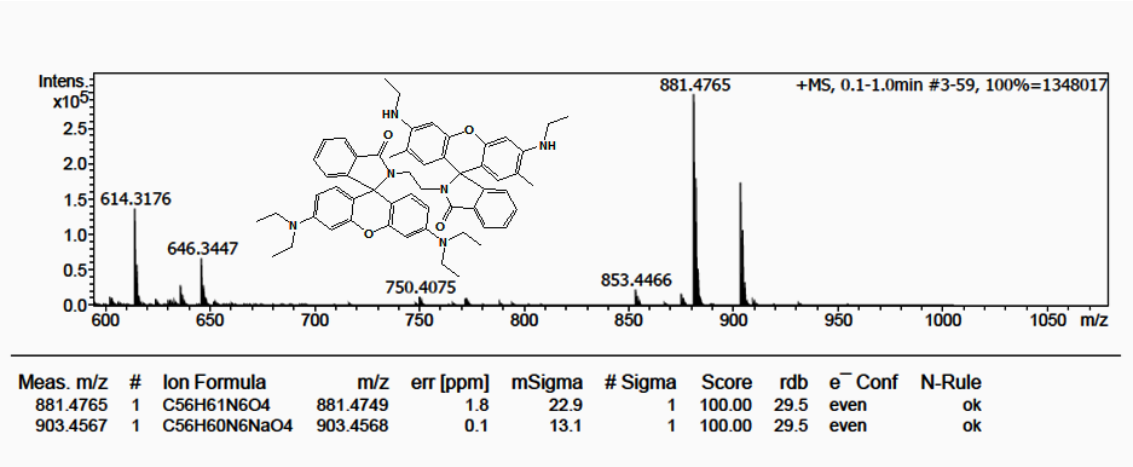

Meas. m/z	#	Ion Formula	m/z	err [ppm]	mSigma	# Sigma	Score	rdb	e⁻ Conf	N-Rule
881.4765	1	C56H61N6O4	881.4749	1.8	22.9	1	100.00	29.5	even	ok
903.4567	1	C56H60N6NaO4	903.4568	0.1	13.1	1	100.00	29.5	even	ok

Fig S32: HR-MS spectrum of **2** (M_w: 880.47).

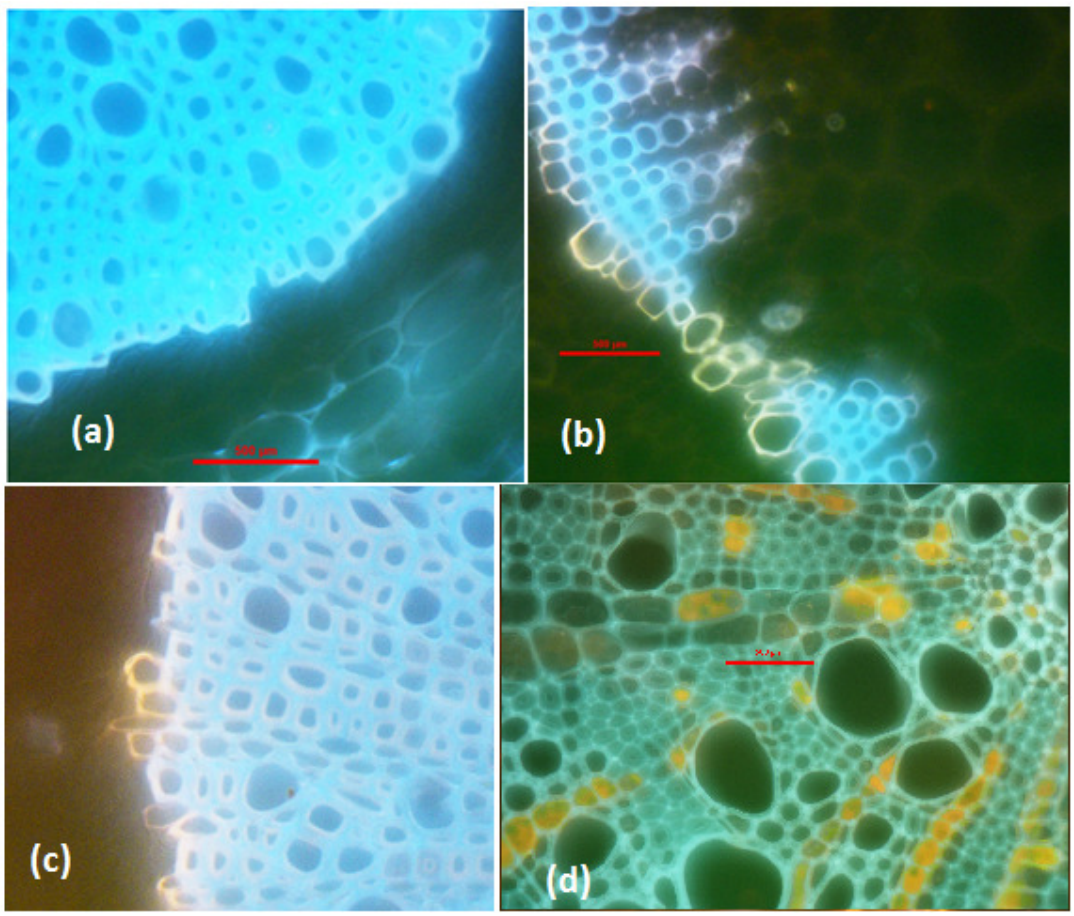

Fig. S33: Fluorescence microscopic images of cross section of *root tissues of G. Pteridifolia* treated with Fe(III) at varying proportions(a) control, (b)10 ppm, (c) 20ppm (d) 30ppm followed by treatment with 1(50 ppm). The bright (orange) emission inferred to Fe(III) deposition on xylem cells.

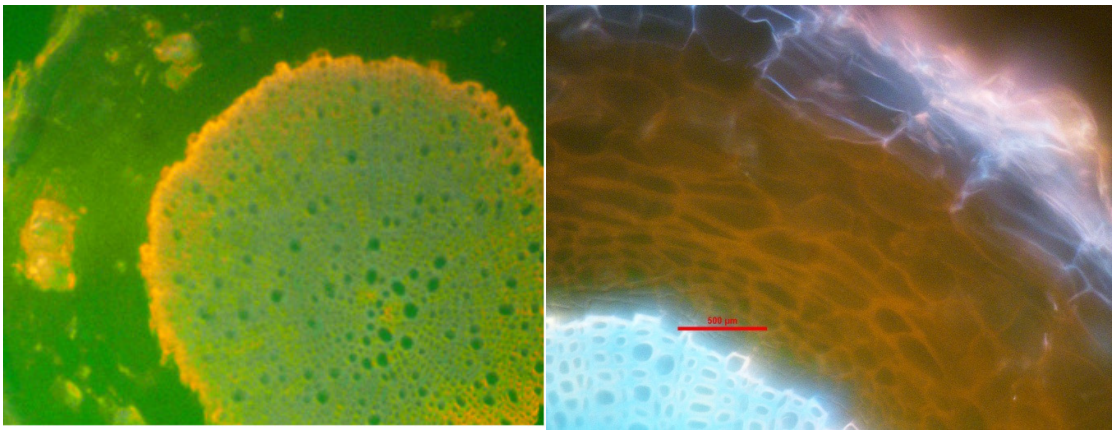

Fig. S34: Fluorescence microscopic images of the cross section of root tissues of *G. Pteridifolia* treated with both Fe(III) ions and **1** at (a) 15mins and (b) after 24h.

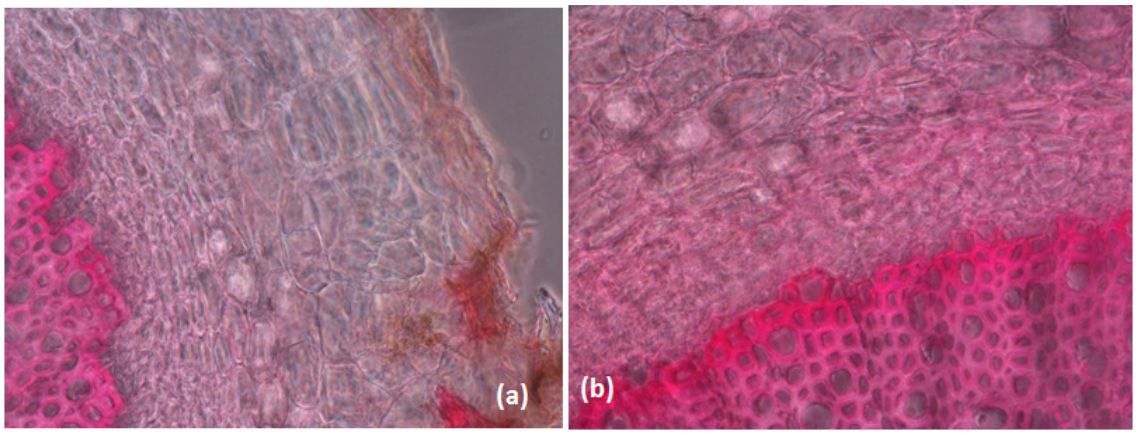

Fig. S35: Microscopic images of the cross section of root tissues of *G. Pteridifolia* treated with both Fe(III) ions and **1** at (a) 15mins and (b) after 24h, showing the colour of **1**-Fe(III) complexes.

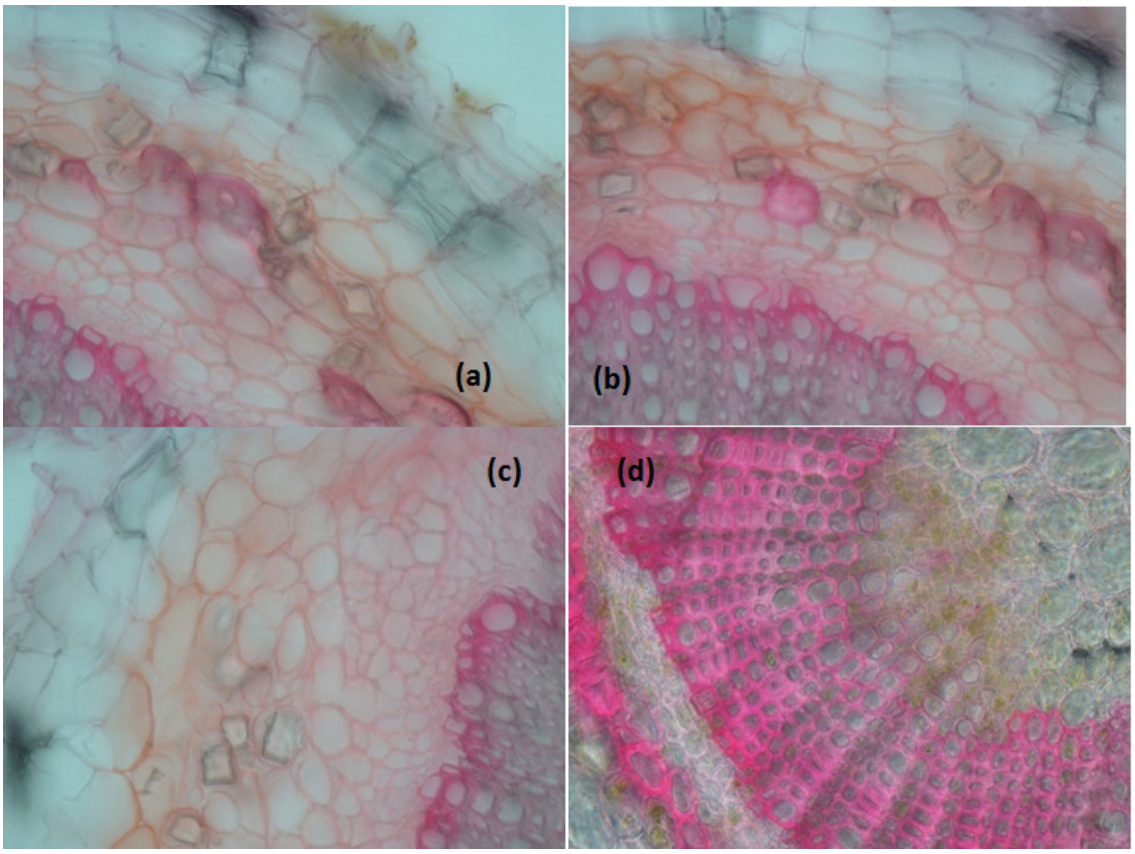

Fig. S36: Microscopic images of the cross section of root tissues of *G. Pteridifolia* treated with Fe(III) ions at varying concentrations (a) 10ppm, (b)20 ppm, (c) 25ppm and (d) 30ppm followed by **1** showing the colour contrast of **1**-Fe(III) complexes.

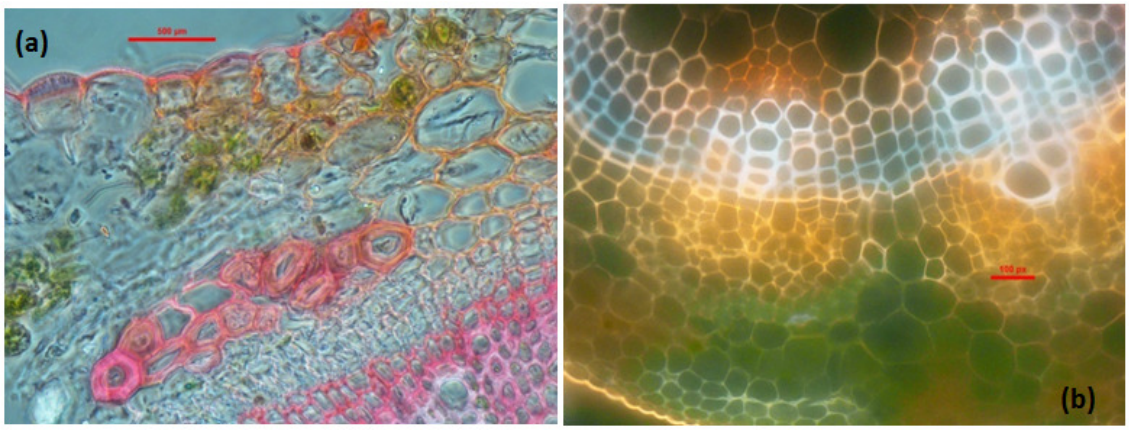

Fig. S37: Fluorescence microscopic images of cross section of stem tissues *of G. Pteridifolia* treated with Fe(III) ion followed by treatment with **1**(50 ppm). The bright (orange) emission inferred to Fe(III) deposition on xylem cells.